mathematics

MDPI

Article

Explicit Non-Traveling Wave Solutions for the (3 + 1)-Dimensional Nonlinear Vakhnenko–Parkes Equation Arising in Fluid Dynamics

Shami A. M. Alsallami

Mathematics Department, College of Sciences, Umm Al-Qura University, Makkah 24381, Saudi Arabia; sasallami@uqu.edu.sa

Abstract

The present work aims to utilize two extended reduction strategies to the (3 + 1)–dimensional nonlinear Vakhnenko–Parkes equation and construct some novel exact non-traveling wave solutions. These approaches transform the main equation into several solvable reduced equations. In each strategy, we first isolate an unconstrained regime of the reduction in which the reduced equation holds identically for an arbitrary smooth reduced function; the exponential, trigonometric, hyperbolic, rational, Jacobi elliptic, and hybrid solution types are then obtained as particular choices of this general family. The solutions obtained from the proposed techniques are expressed in generalized forms that combine exponential, trigonometric, hyperbolic, rational, Jacobi elliptic, and hybrid wave structures. One of the main properties of the constructed solutions is the presence of arbitrary functions, which allows the solutions to possess greater flexibility in describing various phenomena in practical applications. Consequently, the resulting solutions generalize conventional traveling wave solutions and provide a flexible description of non-autonomous and spatially modulated nonlinear wave patterns. The reduction strategies employed generate several families of exact solutions with diverse functional forms. We subsequently include several graphical representations to illustrate the shape of the given solutions. The correctness of all solutions is verified by direct substitution into the governing equation. The proposed framework systematically constructs non-traveling exact solutions for higher-dimensional or variable-coefficient nonlinear evolution equations across diverse physical fields.

Keywords: non-traveling wave solutions; reduction methods; Jacobi elliptic solutions; rational forms; Vakhnenko–Parkes equation

MSC: 35C05; 35C07; 35C08; 35Q51; 37K40

Check for updates

Academic Editor: Imre Ferenc Barna

Received: 7 October 2026
Revised: 4 November 2026
Accepted: 5 November 2026
Published: 8 November 2026

Copyright: © 2026 by the author. Licensee MDPI, Basel, Switzerland. This article is an open access article distributed under the terms and conditions of the Creative Commons Attribution (CC BY) license.

1. Introduction

Nonlinear evolution partial differential equations (NEPDEs) serve as fundamental mathematical tools for modeling diverse physical phenomena in fluid flows, acoustic waves, fiber lasers, and plasmas [1–5]. Finding exact solutions to these equations is therefore of great importance in applied mathematics and physics. Over the past few decades, various analytical methods have been used to derive exact solutions of diverse nonlinear equations. For instance, Hirota's bilinear method [6], Bäcklund transformations [7], expansion methods [8], the generalized exponential rational function method [9], the inverse scattering transform [10], Lie symmetry analysis [11], auxiliary-equation methods, the (G'/G)-expansion method [12], and non-traveling wave reductions [13]. The application of these methods yields a diverse range of exact solutions for the studied nonlinear models,

including solitary waves, periodic waves, breather solutions, and other localized or evolving wave structures.

The $(3+1)$-dimensional Vakhnenko–Parkes equation (VPe) is a nonlinear evolution model for high-frequency wave perturbations in relaxing high-rate active barotropic media. An early version of this model was studied by Vakhnenko in 1992 in the form [14]

$$\frac{\partial}{\partial x}\left(\frac{\partial u}{\partial t}+u\frac{\partial u}{\partial x}\right)+u=0, \tag{1}$$

which describes high-frequency waves in a relaxation medium [15]. Several higher-dimensional extensions of the model were also proposed by Victor et al. [16]

$$\left(\frac{\partial}{\partial x}+\frac{\partial}{\partial y}\right)\left(\frac{\partial}{\partial t}+u\left(\frac{\partial}{\partial x}+\frac{\partial}{\partial y}\right)\right)u+u=0, \tag{2}$$

and by Wazwaz [17]

$$\left(\frac{\partial}{\partial x}+\frac{\partial}{\partial y}+\frac{\partial}{\partial z}\right)\left(\frac{\partial}{\partial t}+u\left(\frac{\partial}{\partial x}+\frac{\partial}{\partial y}+\frac{\partial}{\partial z}\right)\right)u+u=0. \tag{3}$$

Further, using the variable transformations, the author of [18] proposed the following nonlinear VPe:

$$u_{xxt}+u_{xxy}+u_{xxz}+u_tu_x+u_yu_x+u_zu_x+u_x=0, \tag{4}$$

where $u=u(x,y,z,t)$ denotes the dependent variable and the subscripts represent partial derivatives. Equation (3) is the $(3+1)$-dimensional extension of the Vakhnenko–Parkes equation, which models high-frequency wave perturbations in relaxing, high-rate active barotropic media [14,15].

In recent studies, several analytical techniques have been applied to Equation (4). Multiple soliton solutions for the model were obtained using the simplified Hirota method [18]. Moreover, several multi-wave, breather wave, lump-kink, lump-periodic solutions and interaction solutions to the model were obtained in [19]. The modified auxiliary equation approach and the extended (G'/G^2)-expansion method were used in [20] to study the dynamic behavior of the model. The modified auxiliary equation method and the improved F-expansion method were subsequently employed in [21] to derive solitary wave solutions that were combined with periodic waves and rational forms. The Nucci reduction method and an extended direct algebraic approach were also utilized in [22] to construct exact solutions of the governing equation. Beyond exact analytical solutions, Ref. [22] also investigates the qualitative dynamical behavior of the model using bifurcation analysis and phase-plane representations to determine parameter intervals associated with qualitative changes in solution behavior. The multiple exp-function technique was used to construct N-soliton solutions to the model in [23]. Also, a Bäcklund transformation and lump-kink solutions were derived in [24] for a variant of Equation (4). It is notable that conventional traveling wave reductions give solutions that depend on just one phase and a few constants. These forms describe waves propagating in a fixed, rigid manner, lacking the flexibility to adapt when the wave's amplitude, background, phase, or location varies with respect to the remaining independent variables. These considerations motivated us to develop an expanded set of analytical methods capable of yielding solutions with a more general dependence on the independent variables, including non-traveling wave structures. A comparison of the present work with these studies is summarized in Table 1.

The rest of this paper is arranged as follows. In Sections 2 and 3, two extended reduction strategies are introduced to reduce the nonlinear VPe to some simpler forms. The first transformation, Equations (6) and (7), follows our earlier work [25] on a different equation, while the second transformation, Equations (25) and (26), with two reduced variables,

follows the approach of [26]; both are applied here to the VPe. The explicit solution families derived in this work contain arbitrary functions of $z-y$, $t-y$ and $t-z$. In each strategy we present the unconstrained regime in which the reduced equation is satisfied identically by an arbitrary, smooth, reduced function. This produces a general family, and the exponential, trigonometric, hyperbolic, rational, Jacobi elliptic, and hybrid cases then appear as particular choices of the reduced function. Section 4 gives graphical illustrations of selected solutions. Finally, the last section summarizes the main conclusions and possible directions for future investigations of our approach.

Table 1. Comparison with the closest studies of Equation (4).

Ref.	Method	Solutions Obtained	Arbitrary Functions
[18]	Simplified Hirota method	Multiple soliton	No
[19]	Hirota's bilinear form with symbolic computation	Multi-wave, breather, lump-kink, lump-periodic, interaction	No
[20]	Modified auxiliary equation; extended (G'/G^2)-expansion	Traveling wave solutions	No
[21]	Modified auxiliary equation; improved F-expansion	Solitary waves combined with periodic and rational forms	No
[22]	Nucci reduction; extended direct algebraic method	Exact solutions; bifurcation and phase-plane analysis	No
[23]	Multiple exp-function method	N-soliton, front waves	No
[24]	Bäcklund transformation; lump-kink ansatz	Lump-kink solutions (variant of Equation (4))	No
This work	Two reduction strategies, Equations (6), (7), (25) and (26)	General unconstrained family plus selected exponential, trigonometric, hyperbolic, rational, Jacobi elliptic, hybrid profiles	Yes: functions of $z-y$, $t-y$, $t-z$

2. First Reduction Strategy

To derive exact analytical solutions, we first define $\mathcal{D} = \partial_t + \partial_y + \partial_z$. Then, Equation (4) can be written as

$$\mathcal{D}(u_{xx}) + u_x\,(\mathcal{D}u + 1) = 0. \tag{5}$$

Now, we reduce Equation (4) through the following transformation:

$$u(x,y,z,t) = p(y,z,t)\Phi(\xi) + q(x,y,z,t), \tag{6}$$

where the similarity variable ξ is defined by

$$\xi = \varepsilon x + \theta(y,z,t), \tag{7}$$

where $\varepsilon \neq 0$ is a constant parameter. Here, $p(y,z,t)$, $q(x,y,z,t)$, and $\theta(y,z,t)$ are auxiliary functions to be determined, while $\Phi(\xi)$ denotes the reduced dependent variable.

Substituting (6) and (7) into Equation (5) (which is Equation (4) written with $\mathcal{D}$) and applying the chain rule, it is convenient to introduce the abbreviations

$$\omega_3 = \mathcal{D}\theta, \qquad \omega_4 = \mathcal{D}p, \qquad \omega_5 = q_x, \qquad \omega_6 = p.$$

Since $\mathcal{D}x = 0$, we have $\mathcal{D}\xi = \mathcal{D}\theta = \omega_3$, and since $\mathcal{D}t = 1$, the chain rule gives $\mathcal{D}\Phi(\xi) = \omega_3\Phi_\xi$. Therefore,

$$u_x = \varepsilon\omega_6\Phi_\xi + \omega_5, \qquad u_{xx} = \varepsilon^2\omega_6\Phi_{\xi\xi} + q_{xx},$$

$$\mathcal{D}u + 1 = \omega_4\Phi + \omega_6\omega_3\Phi_{\bar{\xi}} + (\mathcal{D}q + 1),$$
$$\mathcal{D}(u_{xx}) = \varepsilon^2[\omega_4\Phi_{\bar{\xi}\bar{\xi}} + \omega_3\omega_6\Phi_{\bar{\xi}\bar{\xi}\bar{\xi}}] + \mathcal{D}q_{xx}.$$

Multiplying u_x by $(\mathcal{D}u + 1)$ gives

$$u_x(\mathcal{D}u + 1) = \varepsilon\omega_4\omega_6\,\Phi\Phi_{\bar{\xi}} + \varepsilon\omega_3\omega_6^2\,\Phi_{\bar{\xi}}^2 + \varepsilon\omega_6(\mathcal{D}q + 1)\,\Phi_{\bar{\xi}} + \omega_4\omega_5\,\Phi + \omega_3\omega_5\omega_6\,\Phi_{\bar{\xi}} + \omega_5(\mathcal{D}q + 1).$$

Adding $\mathcal{D}(u_{xx})$ and collecting the coefficients of Φ and its derivatives, the two $\Phi_{\bar{\xi}}$ terms combine as $\omega_6[\varepsilon(\mathcal{D}q + 1) + q_x\omega_3] = \omega_6\omega_2$, and the terms free of Φ combine as $\mathcal{D}q_{xx} + q_x(\mathcal{D}q + 1) = \omega_1$. Equation (5) thus becomes

$$\varepsilon^2\omega_3\omega_6\Phi_{\bar{\xi}\bar{\xi}\bar{\xi}} + \varepsilon^2\omega_4\Phi_{\bar{\xi}\bar{\xi}} + \omega_6\omega_2\Phi_{\bar{\xi}} + \varepsilon\omega_6^2\omega_3\Phi_{\bar{\xi}}^2 + \varepsilon\omega_6\omega_4\Phi\Phi_{\bar{\xi}} + \omega_5\omega_4\Phi + \omega_1 = 0, \quad (8)$$

where

$$\omega_1 = \mathcal{D}q_{xx} + q_x(\mathcal{D}q + 1), \quad \omega_2 = q_x\mathcal{D}\theta + \varepsilon(\mathcal{D}q + 1), \quad \omega_3 = \mathcal{D}\theta, \quad \omega_4 = \mathcal{D}p, \quad \omega_5 = q_x, \quad \omega_6 = p. \quad (9)$$

Equation (8) provides a reduced equation whose particular form depends on the choice of auxiliary functions.

2.1. General Unconstrained Family

Here, we consider the case in which the reduced equation holds identically for an arbitrary reduced function.

Proposition 1. *If*

$$\omega_1 = \omega_2 = \omega_3 = \omega_4 = 0, \quad (10)$$

then Equation (8) *is satisfied identically for every smooth function* Φ*. Moreover, solving* (10) *together with* (9) *gives*

$$\begin{cases} p(y,z,t) = g_1(z-y,t-y), \\ q(x,y,z,t) = -y + g_2(x,z-y,t-y), \\ \theta(y,z,t) = g_3(z-y,t-y), \end{cases} \quad (11)$$

and hence the following general family of non-traveling solutions of Equation (4)*:*

$$u^{(1)}_{\text{gen}}(x,y,z,t) = g_1(z-y,t-y)\,\Phi(\varepsilon x + g_3(z-y,t-y)) + g_2(x,z-y,t-y) - y, \quad (12)$$

where g_1, g_2, g_3 *are arbitrary sufficiently smooth functions and* Φ *is arbitrary.*

Proof. Under (10), every term in Equation (8) contains at least one of $\omega_1, \omega_2, \omega_3, \omega_4$ as a factor, so Equation (8) is satisfied identically for every smooth Φ. It remains to solve the constraint system (10) together with (9). The equation $\omega_3 = \mathcal{D}\theta = 0$ implies that θ is annihilated by $\mathcal{D} = \partial_t + \partial_y + \partial_z$; its general solution is $\theta = g_3(z-y,t-y)$. Similarly, $\omega_4 = \mathcal{D}p = 0$ gives $p = g_1(z-y,t-y)$. The equation $\omega_2 = q_x\omega_3 + \varepsilon(\mathcal{D}q + 1) = 0$ reduces, using $\omega_3 = 0$, to $\mathcal{D}q = -1$, whose general solution is $q = -y + g_2(x,z-y,t-y)$. Finally, $\omega_1 = \mathcal{D}q_{xx} + q_x(\mathcal{D}q + 1) = \mathcal{D}q_{xx} = 0$ is automatically satisfied because $q_{xx} = (g_2)_{xx}$ is annihilated by $\mathcal{D}$. This yields (11) and, via ansatz (6) and (7), the family in (12). □

2.2. Selected Choices of the Reduced Function Φ

The solutions in this subsection are particular cases of (12). For each example, we state the profile Φ; the auxiliary functions p, q, θ are those of (11) (with the identifications specified in each case).

2.2.1. Exponential Kink-Type Profile

Taking

$$\Phi(\xi) = \frac{c_1 e^{\xi} + c_2}{1 + e^{\xi}}, \tag{13}$$

in (12) gives the kink-type exponential solution

$$u_1(x,y,z,t) = \frac{g_1(z-y,t-y)\left(c_1 e^{\varepsilon x + g_3(z-y,t-y)} + c_2\right)}{1 + e^{\varepsilon x + g_3(z-y,t-y)}} - y + g_2(x,z-y,t-y). \tag{14}$$

(Here, the full three-argument g_2 of (11) is used; in the graphical discussion of Section 4, it is taken independent of x.)

2.2.2. Trigonometric Profile

Taking the constraint $\omega_5 = 1$ (so $q_x = 1$) together with (10), and the profile

$$\Phi(\xi) = c_1 \sin(\xi) + c_2 \cos(\xi), \tag{15}$$

the corresponding family (12) gives

$$u_2(x,y,z,t) = g_1(z-y,t-y)(c_1 \sin(\xi) + c_2 \cos(\xi)) + x - y + g_2(z-y,t-y), \tag{16}$$

where $\xi = \varepsilon x + g_3(z-y,t-y)$, and g_2 in this equation stands for the particular choice $g_2(x,z-y,t-y) = x + \tilde{g}_2(z-y,t-y)$ with $\tilde{g}_2$ relabeled as g_2.

2.2.3. Hyperbolic Profile

Taking $p = 1$ (so $\omega_6 = 1$) together with (10) and

$$\Phi(\xi) = c_1 \operatorname{sech}(\xi) + c_2 \tanh(\xi), \tag{17}$$

we obtain the pulse-kink exact solution

$$u_3(x,y,z,t) = c_1 \operatorname{sech}(\xi) + c_2 \tanh(\xi) - y + g_1(z-y,t-y), \tag{18}$$

where $\xi = \varepsilon x + g_2(z-y,t-y)$. Here, the role of the free functions is: $p \equiv 1$, $q = -y + g_1$, $\theta = g_2$.

2.2.4. Rational Profile

Under the constraints $\omega_1 = \cdots = \omega_5 = 0$ together with

$$\Phi(\xi) = \frac{c_1}{\xi^2 + c_2}, \tag{19}$$

Equations (8) and (9) yield the localized rational solution

$$u_4(x,y,z,t) = \frac{g_1(z-y,t-y)\, c_1}{\left(\varepsilon x + g_3(z-y,t-y)\right)^2 + c_2} - y + g_2(z-y,t-y). \tag{20}$$

For $c_2 > 0$, the denominator is positive for all real arguments, so u_4 is regular wherever g_1, g_2, g_3 are finite. For $c_2 \le 0$, it is singular at $\varepsilon x + g_3 = \pm\sqrt{-c_2}$ and is a solution only on domains that exclude these points. We thus distinguish between a formal exact solution (satisfying Equation (4) wherever it is defined) and a globally regular solution.

2.2.5. Jacobi Elliptic Profile

Taking the profile

$$\Phi(\xi) = c_1 \operatorname{cn}(\xi, m) + c_2 \operatorname{sn}(\xi, m), \tag{21}$$

and replacing the amplitude $g_1(z-y,t-y)$ in (12) by $g_1(z-y,t-y)\,e^{y-t}$, we obtain the Jacobi elliptic solution

$$u_5(x,y,z,t) = g_1(z-y,t-y)e^{y-t}(c_1\,\mathrm{cn}(\xi,m) + c_2\,\mathrm{sn}(\xi,m)) - y + g_2(z-y,t-y), \quad (22)$$

where $\xi = \varepsilon x + g_3(z-y,t-y)$, and m is the elliptic modulus. The arbitrary function g_1 controls the amplitude modulation through the combination $z-y$ and $t-y$, while g_2 provides background deformation, and g_3 determines the phase progression. In the limit $m \to 0$, this solution reduces to a trigonometric form describing linear periodic waves, while in the limit $m \to 1$, it yields hyperbolic localized (sech/tanh-type) structures.

2.2.6. Hybrid Sech-Sin Profile

Taking the profile

$$\Phi(\xi) = \mathrm{sech}(\xi)(\sin(\xi) + c_1\cos(\xi)), \quad (23)$$

the family (12) gives the sech-sin exact solution

$$u_6(x,y,z,t) = g_1(z-y,t-y)\,\mathrm{sech}(\xi)(\sin(\xi) + c_1\cos(\xi)) - y + g_2(z-y,t-y), \quad (24)$$

where $\xi = \varepsilon x + g_3(z-y,t-y)$. This hybrid solution combines localized sech behavior with oscillatory trigonometric modulation, producing a localized oscillatory profile where the arbitrary functions control amplitude, background, and phase.

3. Second Reduction Strategy

To obtain additional classes of exact solutions, we introduce a second extended reduction strategy based on two reduced variables. We consider the transformation

$$u(x,y,z,t) = \Lambda(\xi,\rho) + q(y,z,t), \quad (25)$$

where the reduced variables are defined by

$$\xi = \varepsilon x + \theta(y,t), \qquad \rho = \varepsilon x + \eta(z,t), \quad (26)$$

with $\varepsilon \neq 0$, and where q, θ, and η are auxiliary functions to be determined.

Unlike the first reduction strategy, the present transformation introduces two reduced variables. Consequently, the reduced function $\Lambda(\xi,\rho)$ retains dependence on two combinations of the original independent variables. This additional degree of freedom enables the construction of exact solutions with functional modulation in both reduced directions.

Substituting ansatz (25) into Equation (4) yields the following simplified equation:

$$\varepsilon^2\varrho_1\Lambda_{\xi\xi\rho} + \varepsilon^2\varrho_2\Lambda_{\xi\rho\rho} + \varepsilon\varrho_3\Lambda_\rho\Lambda_\xi + \varepsilon\varrho_4(\Lambda_\xi + \Lambda_\rho) + \varepsilon\varrho_5\left(\Lambda_\xi^2 + \varepsilon\Lambda_{\xi\xi\xi}\right) + \varepsilon\varrho_6\left(\Lambda_\rho^2 + \varepsilon\Lambda_{\rho\rho\rho}\right) = 0, \quad (27)$$

where the coefficients ϱ_i are given by

$$\begin{aligned}
\varrho_1 &= \eta_z + 2\theta_t + \eta_t + 2\theta_y,\\
\varrho_2 &= 2\eta_z + \theta_t + 2\eta_t + \theta_y,\\
\varrho_3 &= \eta_z + \theta_t + \eta_t + \theta_y,\\
\varrho_4 &= q_t + q_y + q_z + 1,\\
\varrho_5 &= \theta_t + \theta_y,\\
\varrho_6 &= \eta_z + \eta_t.
\end{aligned} \quad (28)$$

The derivation of Equation (27) is given in Appendix A.

Different compatible constraints imposed on the coefficient functions in (28) lead to reduced equations of different forms. Two main cases are considered below: a nonzero-coefficient family (Section 3.1) and the unconstrained zero-coefficient regime (Section 3.2), in which all ϱ_i vanish and (27) holds identically for every smooth Λ.

3.1. A Nonzero-Coefficient Family

In accordance with the constraints

$$\varrho_2 = \varrho_4 = 0, \qquad \varrho_5 = 1, \tag{29}$$

Equation (27) together with (28) admits

$$\Lambda(\xi, \rho) = c_1 \sin(2\rho + \xi) + c_2 \cos(2\rho + \xi), \tag{30}$$

and

$$\begin{cases} q(y,z,t) = -y + g_1(z-y, t-y), \\ \theta(y,t) = y + g_2(t-y), \\ \eta(z,t) = -\dfrac{z}{2} + g_3(t-z). \end{cases} \tag{31}$$

As a result, a trigonometric solution to the model is obtained as

$$u_7(x,y,z,t) = c_1 \sin(\Delta) + c_2 \cos(\Delta) - y + g_1(z-y, t-y), \tag{32}$$

where

$$\Delta = 3\varepsilon x - z + 2g_3(t-z) + y + g_2(t-y).$$

This two-variable trigonometric solution exhibits phase modulation through multiple arbitrary functions and demonstrates the versatility of the second reduction strategy.

3.2. General Zero-Coefficient Family

In this part, we consider the regime in which all coefficient functions ϱ_i vanish.

Proposition 2. *If*

$$\varrho_1 = \varrho_2 = \varrho_3 = \varrho_4 = \varrho_5 = \varrho_6 = 0, \tag{33}$$

then Equation (27) *is satisfied identically for every smooth function* $\Lambda(\xi, \rho)$. *Solving* (33) *together with* (28) *gives*

$$\begin{cases} q(y,z,t) = -y + g_1(z-y, t-y), \\ \theta(y,t) = g_2(t-y), \\ \eta(z,t) = g_3(t-z), \end{cases} \tag{34}$$

and hence the following general family of non-traveling solutions of Equation (4)*:*

$$u^{(2)}_{\text{gen}}(x,y,z,t) = \Lambda(\varepsilon x + g_2(t-y),\ \varepsilon x + g_3(t-z)) - y + g_1(z-y, t-y), \tag{35}$$

with arbitrary sufficiently smooth g_1, g_2, g_3 *and arbitrary* Λ.

Proof. Under (33), every term in Equation (27) contains at least one of $\varrho_1, \ldots, \varrho_6$ as a factor, so Equation (27) is satisfied identically for every smooth $\Lambda(\xi, \rho)$. It remains to solve the constraint system (33) together with (28). The equations $\varrho_5 = \theta_t + \theta_y = 0$ and $\varrho_6 = \eta_z + \eta_t = 0$ give $\theta = g_2(t-y)$ and $\eta = g_3(t-z)$. The equation $\varrho_4 = q_t + q_y + q_z + 1 = 0$ gives $q = -y + g_1(z-y, t-y)$. The remaining coefficients $\varrho_1, \varrho_2, \varrho_3$ then vanish automatically, since they are linear combinations of ϱ_5 and ϱ_6. This yields (34) and, via ansatz (25)–(26), the family in (35). □

3.3. Selected Choices of the Reduced Function Λ

All solutions in this subsection are instances of (35), with the auxiliary functions q, θ, η given by (34).

3.3.1. Variable-Coefficient Exponential Profile

Taking

$$\Lambda(\xi,\rho) = f_1(\rho)e^{f_3(\rho)\xi} + f_2(\rho)e^{f_4(\rho)\xi} \tag{36}$$

in (35) gives the variable-coefficient exponential solution

$$u_8(x,y,z,t) = f_1(\rho)e^{f_3(\rho)\xi} + f_2(\rho)e^{f_4(\rho)\xi} - y + g_1(z-y,t-y), \tag{37}$$

where $\xi = \varepsilon x + g_2(t-y)$ and $\rho = \varepsilon x + g_3(t-z)$. With four arbitrary functions $f_1,\ldots,f_4$ of ρ, this solution describes exponentially growing or decaying modes with spatially varying coefficients.

3.3.2. sech^2 Profile

Taking

$$\Lambda(\xi,\rho) = f_1(\rho)\,\mathrm{sech}^2(\xi) + f_2(\rho), \tag{38}$$

in (35) gives the sech^2 solution

$$u_9(x,y,z,t) = f_1(\rho)\,\mathrm{sech}^2(\xi) + f_2(\rho) - y + g_1(z-y,t-y), \tag{39}$$

where $\xi = \varepsilon x + g_2(t-y)$ and $\rho = \varepsilon x + g_3(t-z)$. The amplitude and background are controlled by f_1 and f_2, while the position and width are modulated through g_2 and g_3.

3.3.3. Two-Variable Jacobi Elliptic Profile

Taking

$$\Lambda(\xi,\rho) = f_1(\rho)\,\mathrm{sn}(\xi,m) + f_2(\rho)\,\mathrm{cn}(\xi,m), \tag{40}$$

in (35) gives the two-variable Jacobi elliptic solution

$$u_{10}(x,y,z,t) = f_1(\rho)\,\mathrm{sn}(\xi,m) + f_2(\rho)\,\mathrm{cn}(\xi,m) - y + g_1(z-y,t-y), \tag{41}$$

with $\xi = \varepsilon x + g_2(t-y)$ and $\rho = \varepsilon x + g_3(t-z)$. This extends u_5 by introducing dependence on two reduced variables; the functions f_1,f_2 modulate the amplitudes of sn and cn, while m provides the continuous transition from trigonometric to hyperbolic forms.

3.3.4. Two-Variable Rational Profile

Taking

$$\Lambda(\xi,\rho) = \frac{f_1(\rho)}{\xi^2 + f_2(\rho)}, \tag{42}$$

in (35) gives the two-variable rational solution

$$u_{11}(x,y,z,t) = \frac{f_1(\varepsilon x + g_3(t-z))}{\varepsilon^2x^2 + 2g_2(t-y)\varepsilon x + g_2^2(t-y) + f_2(\varepsilon x + g_3(t-z))} - y + g_1(z-y,t-y). \tag{43}$$

We require $f_2(\rho) > 0$ on the domain considered (equivalently $\xi^2 + f_2(\rho) \neq 0$); if f_2 can vanish or change sign, u_{11} is singular on the set $\xi^2 = -f_2(\rho)$, which must then be excluded. As with u_4, we distinguish between a formal exact solution and a globally regular solution.

3.3.5. Kink-Background Profile

Taking

$$\Lambda(\xi,\rho) = f_1(\rho) + \frac{f_2(\rho)}{1+e^{\xi}}, \tag{44}$$

in (35) gives the kink-background solution

$$u_{12}(x,y,z,t) = f_1(\varepsilon x + g_3(t-z)) + \frac{f_2(\varepsilon x + g_3(t-z))}{1+e^{\varepsilon x + g_2(t-y)}} - y + g_1(z-y,t-y). \tag{45}$$

Since $1 + e^{\xi} > 0$ for real ξ, neither u_{12} nor u_1 has a singularity coming from its denominator wherever the functions involved are finite.

Remark 1. *The correctness of the derived solutions is verified by direct substitution into the main equation. Moreover, detailed substitutions for u_2 and u_7 are given in Appendix B.*

Remark 2. *Table 2 summarizes the relative merits and drawbacks of the two strategies employed in this paper. The first uses a single reduced variable and gives a simple ordinary reduced equation with explicit constraints but permits modulation in only one direction; the second uses two reduced variables and allows modulation in two directions, at the cost of more constraints, ansatz-based solutions and a less direct interpretation.*

Table 2. Comparison of the two reduction strategies.

	First Strategy	**Second Strategy**
Reduced variables	One: $\xi = \varepsilon x + \theta(y,z,t)$	Two: ξ and ρ
Reduced equation	Equation (8), simple to analyze	Equation (27), PDE in two variables
General family	Equation (12), Φ arbitrary	Equation (35), Λ arbitrary
Merits	Explicit constraints; arbitrary functions of $(z-y, t-y)$ control amplitude, background and phase	Modulation in two directions; additional arbitrary functions $f_i(\rho)$
Drawbacks	Only one reduced phase; few free constants (c_1, c_2, ε)	More constraints; solutions come from ansatz forms, not a general solution; harder interpretation

4. Graphical Representation of Selected Solutions

In this section, we present graphical visualizations of selected exact solutions. No numerical solver for the PDE was used: the figures are plots of the closed-form expressions obtained in Sections 2 and 3, evaluated for selected parameters and arbitrary functions.

4.1. Exponential Kink-Type Solution u_1

The exponential kink-type solution u_1 given by Equation (14) represents a smooth transition layer with variable amplitude and background. The factor g_1 modulates height and steepness, g_2 provides an additive background deformation, and g_3 controls the position of the kink front through $\xi = \varepsilon x + g_3(z-y, t-y)$. Figure 1 presents several plots of this solution when the fixed parameters are taken as

$$\varepsilon = 1, \qquad c_1 = 2, \qquad c_2 = 1, \qquad x = 1, \qquad y = 0, \tag{46}$$

and three different choices of arbitrary functions (with g_2 taken independent of x, as noted in Section 2.2.1):

$$\begin{aligned}
(a)\quad & g_1(r,s) = 0.5\cos(r) + 0.3\sin(s),\\
& g_2(x,r,s) = 0.4e^{x-0.5r^2} + 0.2\cos(x+s),\\
& g_3(r,s) = 0.6r + 0.5\sin(0.8s),\\
(b)\quad & g_1(r,s) = 0.7e^{-0.3(r^2+s^2)} + 0.2,\\
& g_2(x,r,s) = 0.5\tanh(x+0.4r) + 0.3\cos(x+1.2s),\\
& g_3(r,s) = 0.4r + 0.6\sin(s),\\
(c)\quad & g_1(r,s) = \frac{0.6}{1+0.2r^2} + 0.3\cos(s),\\
& g_2(x,r,s) = 0.3\sin(x+r) + 0.4\cos^2(x+s),\\
& g_3(r,s) = 0.5r + 0.7\sin(0.6s).
\end{aligned} \tag{47}$$

In case (a), the exponential and trigonometric combination produces a localized amplitude modulation with an oscillatory background. In case (b), the Gaussian amplitude creates a localized kink with saturating envelope. In case (c), the rational decay generates algebraic localization with trigonometric corrections affecting the kink position and shape. Figure 2 also depicts the cross-sectional behavior of u_1.

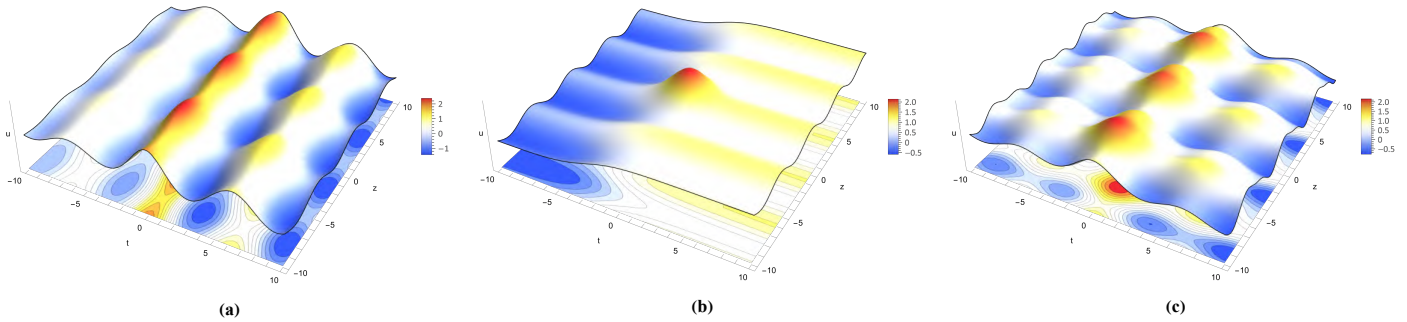


Figure 1. Three-dimensional representation of u_1 when (46) and free functions (47) are considered. The subfigures (**a**–**c**) illustrate cases (a)–(c) of (47), respectively.

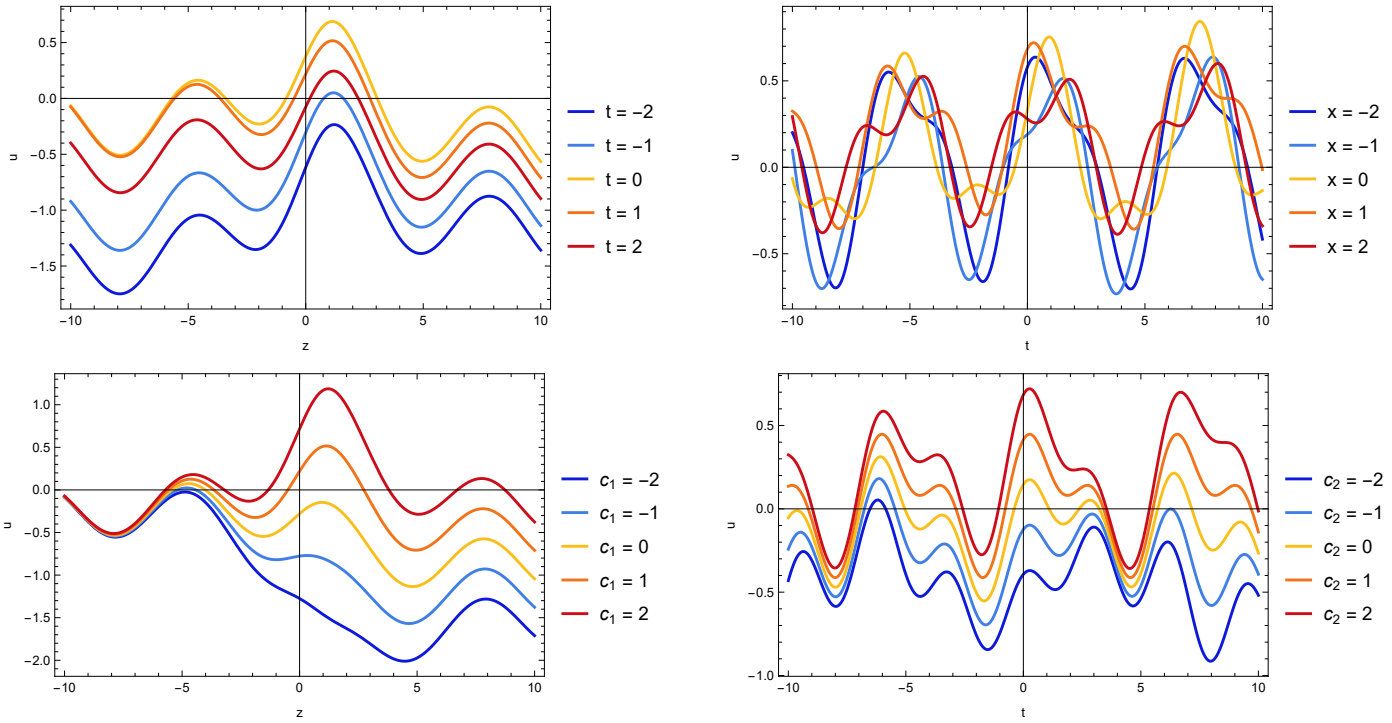


Figure 2. Different cross-sections of u_1 using case (c) in (47) with the fixed parameters of (46). (**First row**): u versus z at fixed t, u versus t at fixed x. (**Second row**): Sensitivity of the solution to c_1 (u versus z) and to c_2 (u versus t).

4.2. Trigonometric Solution u_2

The trigonometric solution u_2 given by Equation (16) is a modulated wave train with a linear drift: its oscillations are governed by sine and cosine functions of $\xi = \varepsilon x + g_3(z - y, t - y)$, where g_3 provides nonlinear phase modulation. The amplitude is set by g_1, the linear background drift comes from $x - y$, and g_2 adds an additive deformation. Figure 3 presents several representations of this solution for the fixed parameters (46) and three different choices of arbitrary functions:

$$
\begin{aligned}
(a)\quad & g_1(r,s) = 0.7\cos(1.2r) + 0.3\sin(0.8s),\\
& g_2(r,s) = 0.5\sin(0.6r + 0.4s) + 0.2\cos(1.5s),\\
& g_3(r,s) = 0.8r + 0.6\sin(1.1s),\\
(b)\quad & g_1(r,s) = 0.6(1 - e^{-0.4s^2}) + 0.3\cos(r),\\
& g_2(r,s) = 0.4\sin(1.3r)\cos(0.7s),\\
& g_3(r,s) = 0.5r + 0.8\sin(0.9s) + 0.3\cos(r),\\
(c)\quad & g_1(r,s) = 0.5\sin(r)\cos(1.2s) + 0.3\cos(0.8r + s),\\
& g_2(r,s) = 0.6\cos^2(1.1r) + 0.3\sin(1.4s),\\
& g_3(r,s) = 0.7r + 0.5\sin(0.8s) + 0.4\cos(0.6r).
\end{aligned}
\tag{48}
$$

In case (a), sine and cosine terms are combined with varying frequencies, which results in a wave train with regular periodic modulation. In case (b), g_1 is characterized by a saturating exponential envelope that modulates a wave train with a smooth onset. In case (c), the product and sum of trigonometric terms generate quasi-periodic patterns across several frequencies, leading to a complex modulation landscape. The cross-sectional behavior of u_2 is also presented in Figure 4.

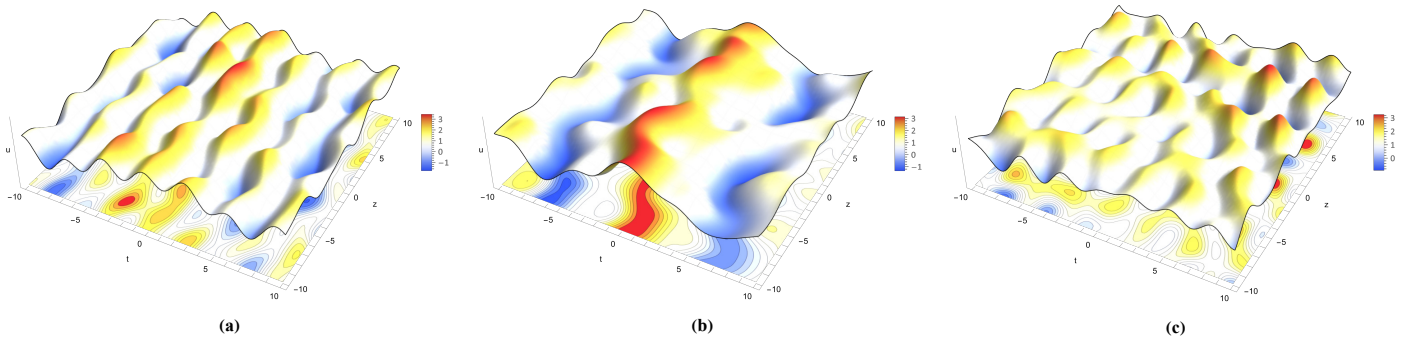


Figure 3. Three-dimensional representation of u_2 when (46) and free functions (48) are considered. The plots in panels (**a**–**c**) are associated with cases (a)–(c) of (48), respectively.

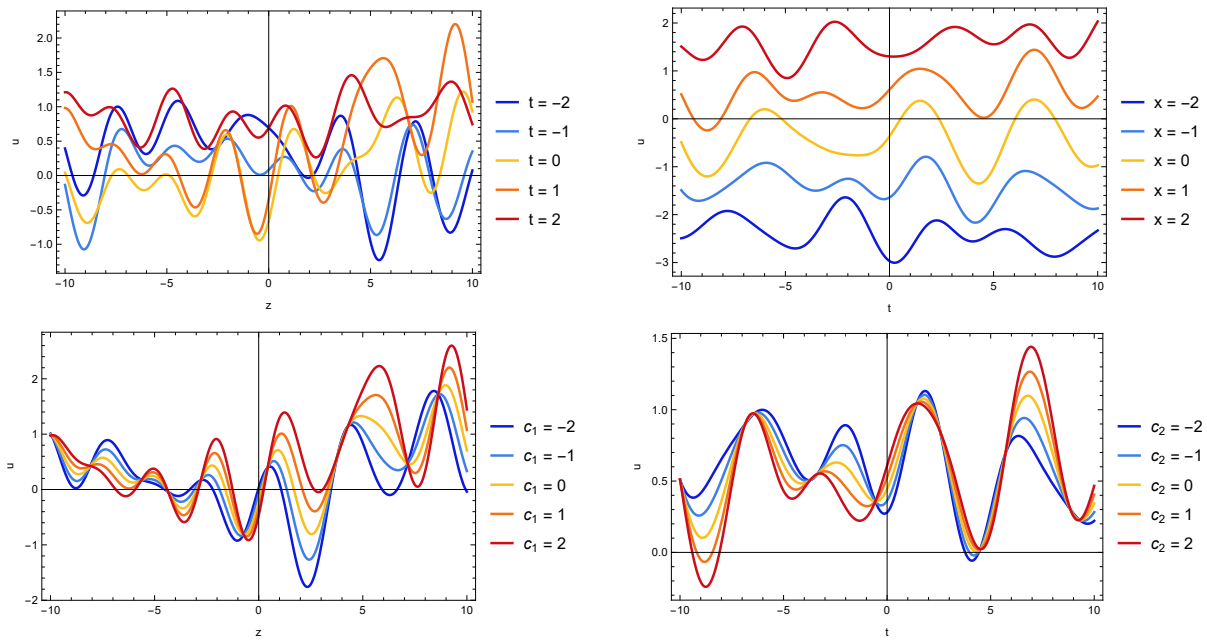


Figure 4. Different cross-sections of u_2 using case (c) in (48) with the fixed parameters of (46). (**First row**): u versus z at fixed t, u versus t at fixed x. (**Second row**): Sensitivity of the solution to c_1 (u versus z) and to c_2 (u versus t).

4.3. Hyperbolic Pulse-Kink Solution u_3

The hyperbolic solution u_3 given by Equation (18) represents a modulated pulse–kink wave structure. The positive value of c_1 produces a localized pulse through the $\operatorname{sech}(\xi)$ term, while $c_2 \tanh(\xi)$ creates a smooth kink-type transition. The arbitrary function g_2 modulates the effective wave coordinate, producing a non-rigid deformation of the wave profile, while g_1 controls the background deformation. The profile combines a localized pulse with a kink-type background (a statement about its shape only). Figure 5 presents several representations for the fixed parameters (46) and three different choices of arbitrary functions:

$$\begin{aligned} (a) \quad & g_1(r,s) = 0.7\cos(r) - 0.2\sin(s), \\ & g_2(r,s) = 0.3\sin(r) + 0.5\cos(s), \\ (b) \quad & g_1(r,s) = 1 - e^{-0.5s^2}, \\ & g_2(r,s) = 1.1\sin(0.8r) + 0.7\cos(s), \\ (c) \quad & g_1(r,s) = e^{-0.7r^2}, \\ & g_2(r,s) = 0.5\cos^2(r) + 0.4\sin^2(s). \end{aligned} \tag{49}$$

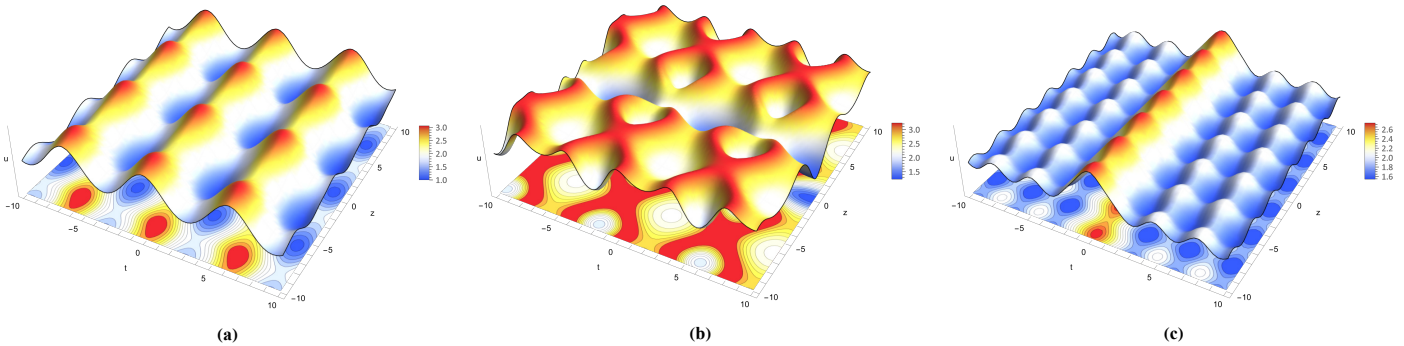


Figure 5. Three-dimensional representation of u_3 when (46) and free functions (49) are considered. Each subfigure (**a**–**c**) corresponds to the respective case (a)–(c) of (49).

Case (a): g_1 and g_2 are periodic sums of sine and cosine, giving a regular oscillatory modulation of the pulse-kink with recurring amplitude changes. Case (b): g_1 adds a smooth saturating background via $1-e^{-0.5s^2}$, while g_2 combines a cosine with an offset, producing an asymmetric kink modulation. Case (c): g_1 is a Gaussian $e^{-0.7r^2}$ that localizes the background, and g_2 uses squared trig terms to yield a positive, ripple-like modulation of the carrier. Furthermore, the parametric study of u_3 is illustrated in Figure 6. In this demonstration, the top row presents the evolution of the solution with respect to the spatial coordinates z and t, while the bottom row shows the sensitivity of the solution to the constants c_1 and c_2.

4.4. Hybrid Sech-Sin Solution u_6

The hybrid sech-sin solution u_6 given by Equation (24) combines localized sech behavior with oscillatory trigonometric modulation through the expression $\operatorname{sech}(\xi)(\sin(\xi) + c_1\cos(\xi))$. This structure produces a localized profile with internal carrier oscillations. Figure 7 presents several representations for the fixed parameters

$$\varepsilon = 0.5, \qquad c_1 = 2, \qquad x = 1, \qquad y = 1, \tag{50}$$

and three different choices of arbitrary functions:

$$
\begin{aligned}
(a)\quad & g_1(r,s) = 0.5\cos(r) + 0.3\sin(s),\\
& g_2(r,s) = 0.4\sin(r) + 0.2\cos(s),\\
& g_3(r,s) = 0.6r + 0.5\sin(s),\\
(b)\quad & g_1(r,s) = 0.7e^{-0.2r^2} + 0.2,\\
& g_2(r,s) = 0.5\tanh(0.3r) + 0.3\cos(s),\\
& g_3(r,s) = 0.5r + 0.6\sin(0.8s),\\
(c)\quad & g_1(r,s) = \frac{0.6}{1+0.2r^2} + 0.3\sin(s),\\
& g_2(r,s) = 0.3\cos(r) + 0.4\sin^2(s),\\
& g_3(r,s) = 0.4r + 0.7\sin(0.6s).
\end{aligned}
\tag{51}
$$

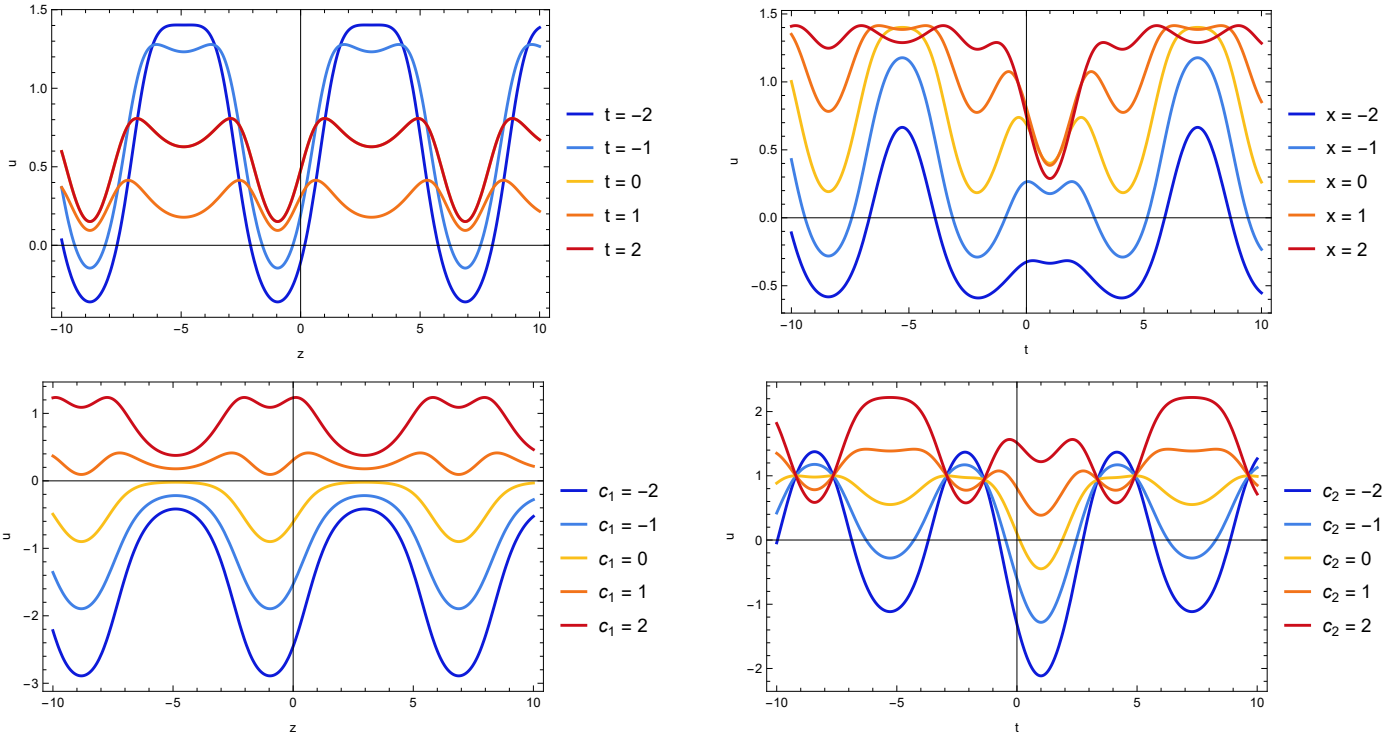


Figure 6. Different cross-sections of u_3 using case (b) in (49) with the fixed parameters of (46). (**First row**): u versus z at fixed t, u versus t at fixed x. (**Second row**): Sensitivity of the solution to c_1 (u versus z) and to c_2 (u versus t).

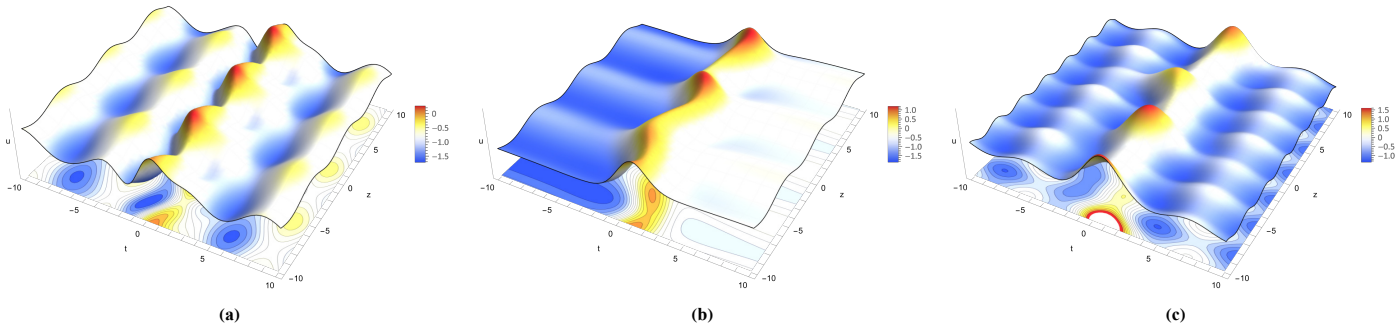


Figure 7. Three-dimensional representation of u_6 when (50) and free functions (51) are considered. Panels (**a**–**c**) correspond to cases (a)–(c) of (51), respectively.

Case (a) yields a regular oscillatory profile formed by purely oscillatory components. Case (b) features a localized envelope structure, produced by an exponential envelope super-

imposed on a background deformation. Case (c) exhibits algebraic localization from rational decay. Figure 8 illustrates the sensitivity of the solution u_6 to its variables and parameters.

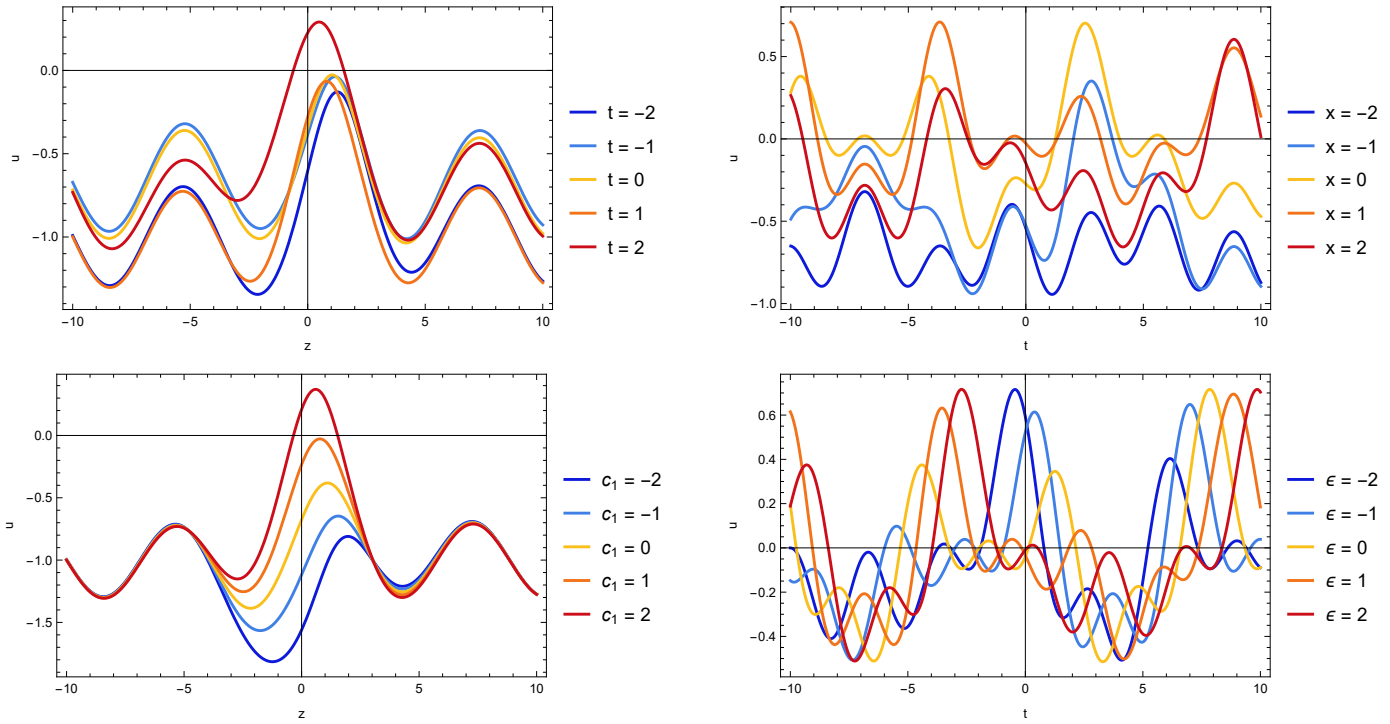


Figure 8. Different cross-sections of u_6 using case (c) in (51) with the fixed parameters of (50). (**First row**): u versus z at fixed t, u versus t at fixed x. (**Second row**): Sensitivity of the solution to c_1 (u versus z) and to ε (u versus t).

4.5. Two-Variable Trigonometric Solution u_7

The two-variable trigonometric solution u_7 given by Equation (32) represents a modulated wave train whose phase depends on both reduced variables through $\Delta = 3\varepsilon x - z + 2g_3(t-z) + y + g_2(t-y)$. The term $-y + g_1(z-y, t-y)$ provides a background deformation, while the trigonometric terms generate oscillatory behavior with a phase that evolves nontrivially in space and time. Figure 9 presents several representations for the fixed parameters

$$\varepsilon = 0.7, \qquad c_1 = 2, \qquad c_2 = 1, \qquad x = 0.6, \qquad y = 0.8, \tag{52}$$

and three different choices of arbitrary functions (with g_2, g_3 one-variable, as required by (31)):

$$\begin{aligned}
(a)\quad & g_1(r,s) = 0.5\cos(r) + 0.3\sin(s),\\
& g_2(r) = 0.4\sin(r) + 0.2\cos(r),\\
& g_3(r) = 0.6r + 0.5\sin(r),\\
(b)\quad & g_1(r,s) = 0.7e^{-0.2r^2} + 0.2,\\
& g_2(r) = 0.5\tanh(0.3r) + 0.3\cos(r),\\
& g_3(r) = 0.5r + 0.6\sin(0.8r),\\
(c)\quad & g_1(r,s) = \frac{0.6}{1+0.2r^2} + 0.3\sin(s),\\
& g_2(r) = 0.3\cos(r) + 0.4\sin^2(r),\\
& g_3(r) = 0.4r + 0.7\sin(0.6r).
\end{aligned} \tag{53}$$

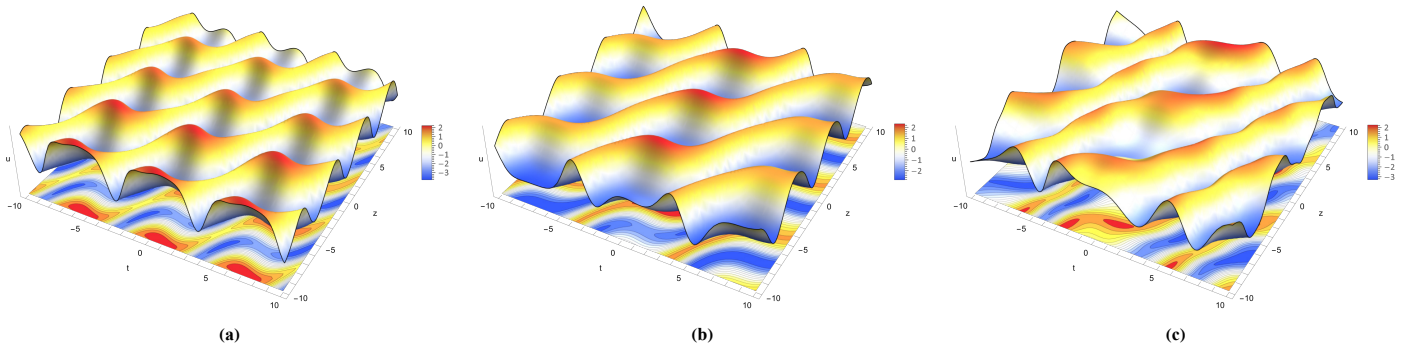


Figure 9. Three-dimensional representation of u_7 when (52) and free functions (53) are considered. Panels (**a**–**c**) correspond to cases (a)–(c) of (53), respectively.

These choices for g_1, g_2, and g_3 illustrate the effect of the arbitrary functions on the two-variable trigonometric solution. In case (a), the purely oscillatory functions produce a regular wave train with periodic phase modulation. In case (b), the exponential amplitude creates a localized envelope with a smooth background, while the hyperbolic tangent introduces a transition in the background deformation. In case (c), the rational decay generates algebraic localization with oscillatory corrections affecting the phase structure. Further, as illustrated in Figure 10, we investigate the solution's dependence on its parameters and independent variables. The top-left panel presents the spatial profiles along z at fixed time slices $t = -2, -1, 0, 1, 2$, revealing the oscillatory structure of the profiles across the domain. The top-right panel displays the temporal evolution along t at fixed y values $y = -2, -1, 0, 1, 2$, illustrating how the wave amplitude varies with the coordinate y. The bottom-left panel demonstrates the influence of constant c_1 on the solution profile, and the bottom-right panel explores the effect of constant c_2 on the evolution of u_7.

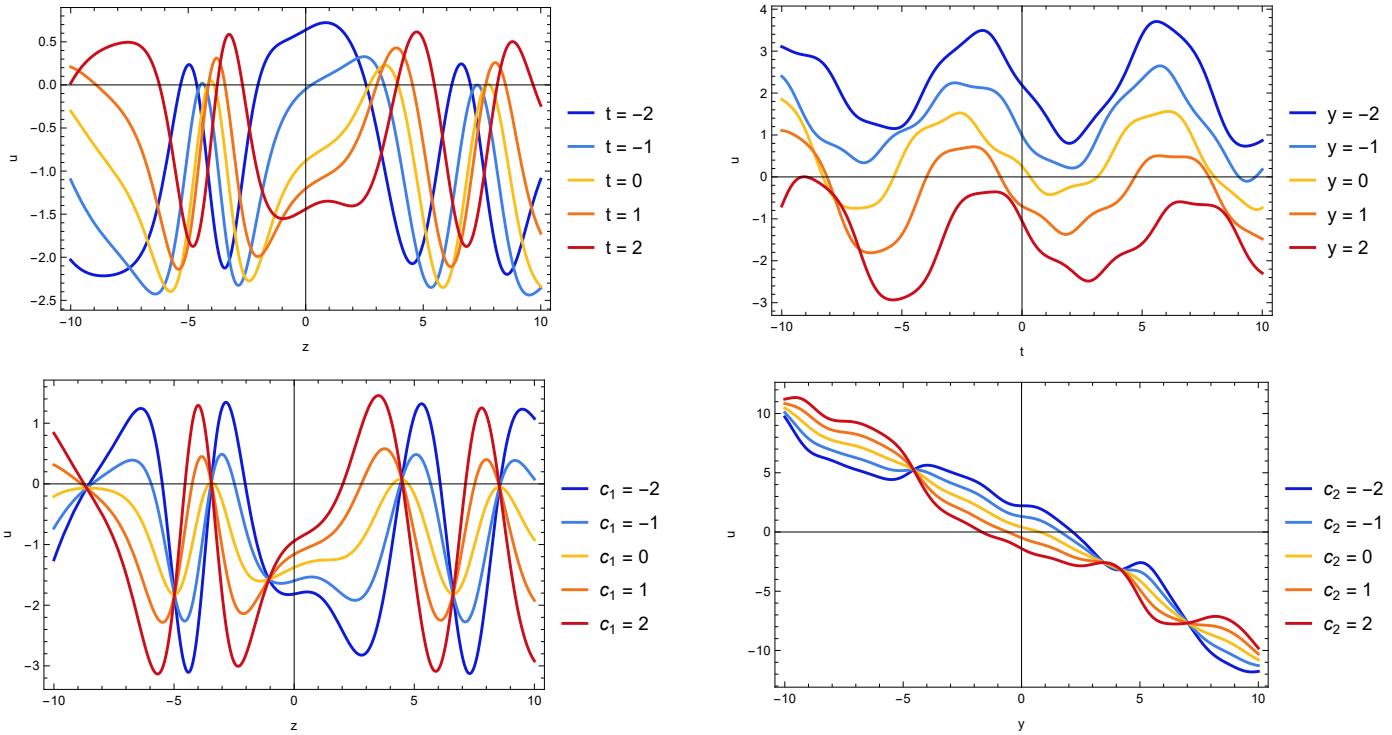


Figure 10. Different cross-sections of u_7 using case (a) in (53) with the fixed parameters of (52). (**First row**): u versus z at fixed t, u versus t at fixed y. (**Second row**): Sensitivity of the solution to c_1 (u versus z) and to c_2 (u versus y).

4.6. sech² Solution u_9

The sech² solution u_9 given by Equation (39) represents a localized profile whose amplitude and background are independently modulated through $f_1(\rho)$ and $f_2(\rho)$, while the phase dynamics are controlled by $g_2(t-y)$ and $g_3(t-z)$. The term $f_1(\rho)\,\mathrm{sech}^2(\xi)$ generates a localized pulse with variable amplitude, where $\xi = \varepsilon x + g_2(t-y)$ determines the position and width, and $\rho = \varepsilon x + g_3(t-z)$ governs the amplitude modulation through f_1 and f_2. The background deformation is provided by $-y + g_1(z-y, t-y)$. Figure 11 presents several representations for the fixed parameters

$$\varepsilon = 1, \qquad x = 1, \qquad y = 0, \tag{54}$$

and three different choices of the arbitrary functions (with g_2, g_3 one-variable):

$$\begin{aligned}
(a)\quad & f_1(\rho) = 1 + \sin(\rho), \quad f_2(\rho) = \cos(\rho),\\
& g_1(r,s) = \sin(r+s),\\
& g_2(r) = \sin(r) + \cos(r), \quad g_3(r) = \sin(r) + \cos(r),\\
(b)\quad & f_1(\rho) = e^{-\rho^2}, \quad f_2(\rho) = 0.5e^{-\rho^2},\\
& g_1(r,s) = \tanh(r),\\
& g_2(r) = \sin(r), \quad g_3(r) = \cos(r),\\
(c)\quad & f_1(\rho) = \frac{1}{1+\rho^2}, \quad f_2(\rho) = \frac{0.5}{1+\rho^2},\\
& g_1(r,s) = \cos(s) + \sin(r),\\
& g_2(r) = \cos(r) + \sin(r), \quad g_3(r) = \cos(r) + \sin(r).
\end{aligned} \tag{55}$$

These forms of f_1, f_2, g_1, g_2, and g_3 illustrate the effect of the arbitrary functions on the sech² solution. In case (a), the oscillatory functions produce a localized pulse with periodically varying amplitude and background. In case (b), the Gaussian modulations create a localized envelope with smooth background variations. In case (c), the rational decay generates algebraic modulations with oscillatory corrections affecting the amplitude and position of the pulse. Further, as illustrated in Figure 12, we investigate the solution's dependence on its key parameters and independent variables.

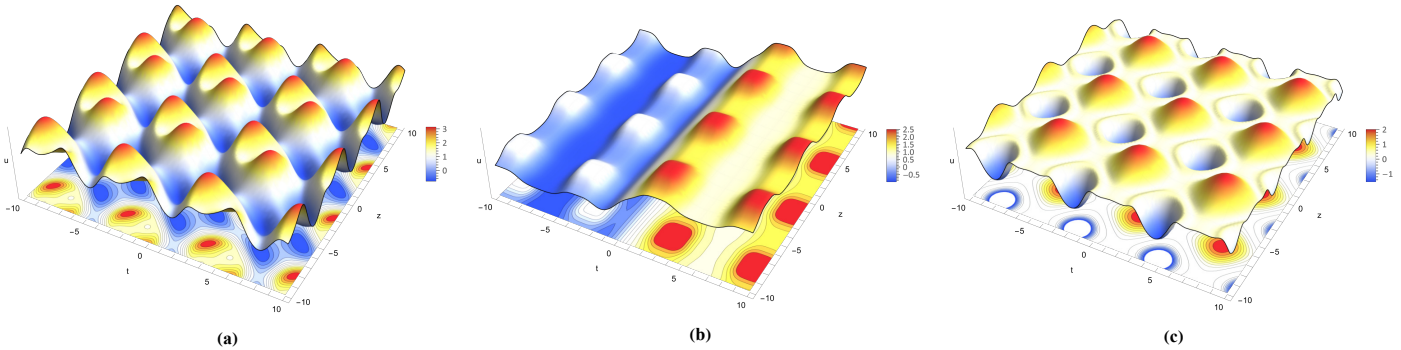


Figure 11. Three-dimensional representation of u_9 when (54) and free functions (55) are considered. The plots in panels (**a**–**c**) are associated with cases (a)–(c) of (55), respectively.

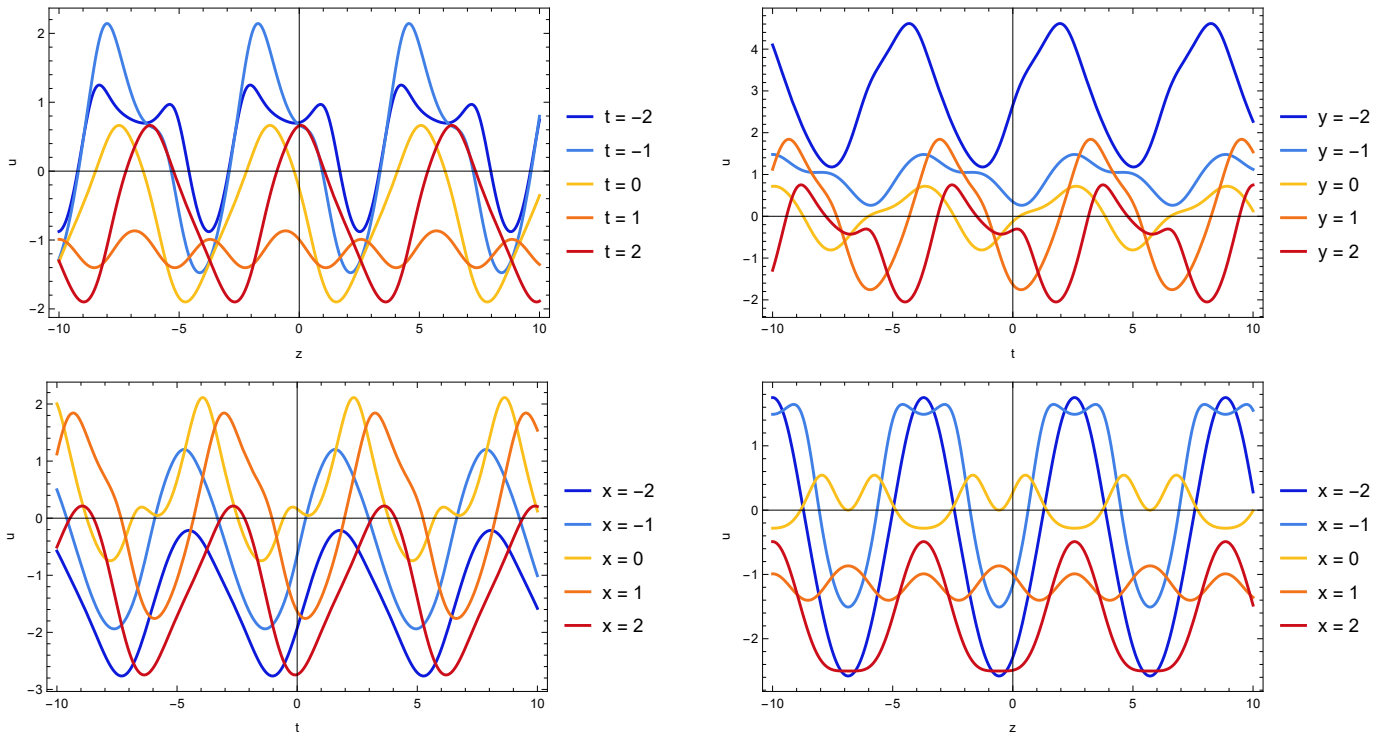


Figure 12. Different cross-sections of u_9 using case (a) in (55) with the fixed parameters of (54). (**First row**): u versus z at fixed t, u versus t at fixed y. (**Second row**): u versus t at fixed x, u versus z at fixed x.

5. Conclusions

In this work, we developed a systematic framework for constructing exact non-traveling wave solutions of the $(3+1)$-dimensional nonlinear Vakhnenko–Parkes equation. Two extended reduction strategies were introduced to reduce the governing multidimensional equation into tractable reduced equations while preserving dependence on combinations of the original independent variables. In each strategy we first identified the unconstrained regime in which the reduced equation held identically for an arbitrary smooth reduced function; this yielded the general families (12) and (35). The exponential, trigonometric, hyperbolic, rational, Jacobi elliptic, and hybrid solution types were particular choices of the reduced function within these families (with the exception of u_7, which used nonzero ϱ_i).

The exact solutions obtained from the two reduction strategies exhibited several distinct functional structures. From the first strategy, we obtained exponential kink-type, trigonometric, hyperbolic pulse-kink, rational localized, Jacobi elliptic, and hybrid sech-sin solutions. From the second strategy, we obtained two-variable trigonometric, variable-coefficient exponential, sech^2, two-variable Jacobi elliptic, two-variable rational, and kink-background solutions.

A distinguishing feature of the constructed solutions is the presence of arbitrary functions of combinations of the independent variables, such as $z-y$, $t-y$, $t-z$, and corresponding combinations appearing in the second reduction. The arbitrary functions appearing in the solutions must be selected according to the physical boundary or initial conditions of the problem under consideration. The results demonstrate that the proposed reduction framework is effective and systematic for constructing generalized exact solutions of higher-dimension nonlinear evolution equations. The employed reduction strategies and their possible extensions provide an efficient way for constructing more general exact solutions of diverse nonlinear evolution equations. Since the solutions contain arbitrary functions, no single stability result applies to them. A stability analysis, whether linear

or by direct numerical simulation of the full nonlinear VPe (4), requires fixing specific functions, boundary and initial data, and a class of perturbations, and remains a direction for future work.

Funding: The author received no funding for this work.

Data Availability Statement: The original contributions presented in this study are included in the article. Further inquiries can be directed to the corresponding author.

Acknowledgments: The author thanks the editor and the reviewers for their careful reading and constructive comments, which greatly improved the clarity and presentation of this work.

Conflicts of Interest: The author declares no conflicts of interest.

Abbreviations and Symbols

The following abbreviations and symbols are used in this manuscript:

NEPDE	Nonlinear evolution partial differential equation
VPe	Vakhnenko–Parkes equation
$\mathcal{D}$	Operator $\partial_t + \partial_y + \partial_z$
ε	Nonzero constant in the similarity variables
ξ, ρ	Reduced (similarity) variables
Φ, Λ	Reduced dependent variables (first/second strategy)
p, q, θ, η	Auxiliary functions in the transformations
ω_j, ϱ_i	Coefficient functions of the reduced equations
g_i, f_i	Arbitrary functions
c_1, c_2	Constants
m	Elliptic modulus
sn, cn	Jacobi elliptic functions
sech, tanh	Hyperbolic secant and tangent
Δ	Phase of u_7, $\Delta = 3\varepsilon x - z + 2g_3(t-z) + y + g_2(t-y)$

Appendix A. Derivation of Equation (27)

Equation (27). Let $u = \Lambda(\xi, \rho) + q$, $\xi = \varepsilon x + \theta(y,t)$, $\rho = \varepsilon x + \eta(z,t)$. Then, $u_x = \varepsilon(\Lambda_\xi + \Lambda_\rho)$, $\mathcal{D}\xi = \theta_t + \theta_y = \varrho_5$, $\mathcal{D}\rho = \eta_z + \eta_t = \varrho_6$ and $\mathcal{D}u + 1 = \varrho_5\Lambda_\xi + \varrho_6\Lambda_\rho + \varrho_4$. Hence,

$$\mathcal{D}(u_{xx}) = \varepsilon^2[\varrho_5(\Lambda_{\xi\xi\xi} + 2\Lambda_{\xi\xi\rho} + \Lambda_{\xi\rho\rho}) + \varrho_6(\Lambda_{\xi\xi\rho} + 2\Lambda_{\xi\rho\rho} + \Lambda_{\rho\rho\rho})], \tag{A1}$$

$$u_x(\mathcal{D}u + 1) = \varepsilon[\varrho_5\Lambda_\xi^2 + \varrho_6\Lambda_\rho^2 + (\varrho_5 + \varrho_6)\Lambda_\xi\Lambda_\rho + \varrho_4(\Lambda_\xi + \Lambda_\rho)]. \tag{A2}$$

Collecting terms gives Equation (27) with $\varrho_1 = 2\varrho_5 + \varrho_6$, $\varrho_2 = \varrho_5 + 2\varrho_6$, $\varrho_3 = \varrho_5 + \varrho_6$, in agreement with Equation (28).

Appendix B. Detailed Verification of Representative Solutions

u_2 (first strategy). Let $\xi = \varepsilon x + g_3$ and $\Phi = c_1 \sin\xi + c_2 \cos\xi$, with $g_i = g_i(z-y, t-y)$, and $u_2 = g_1\Phi + x - y + g_2$. Then, $u_x = \varepsilon g_1\Phi_\xi + 1$ and $u_{xx} = \varepsilon^2 g_1\Phi_{\xi\xi}$. Since $\mathcal{D}g_i = 0$ and $\mathcal{D}\xi = 0$, we get $\mathcal{D}(u_{xx}) = 0$. Moreover, $\mathcal{D}u = \mathcal{D}(x-y) = -1$, so $\mathcal{D}u + 1 = 0$, and (5) holds identically.

u_7 (second strategy). Let $\Delta = 3\varepsilon x - z + y + 2g_3(t-z) + g_2(t-y)$ and $u_7 = c_1 \sin\Delta + c_2\cos\Delta - y + g_1(z-y, t-y)$. Then, $\mathcal{D}\Delta = -1+1+0+0 = 0$, because $\mathcal{D}(t-z) = \mathcal{D}(t-y) = 0$. Hence, $u_{xx} = -9\varepsilon^2(c_1\sin\Delta + c_2\cos\Delta)$ has $\mathcal{D}(u_{xx}) = 0$, and $\mathcal{D}u = \mathcal{D}(-y) = -1$, so $\mathcal{D}u + 1 = 0$. In terms of Equation (27): $\varrho_5 = 1$, $\varrho_6 = -\frac{1}{2}$, $\varrho_4 = 0$, hence $\varrho_1 = \frac{3}{2}$, $\varrho_2 = 0$, $\varrho_3 = \frac{1}{2}$, and with $\Lambda = F(2\rho + \xi)$, the F'^2 terms cancel $(1 + 1 - 2 = 0)$, and the F''' terms cancel $(3 + 1 - 4 = 0)$, so Equation (27) is satisfied.

References

1. Logan, J.D. *An Introduction to Nonlinear Partial Differential Equations*; John Wiley & Sons: Hoboken, NJ, USA, 2008.

2. Ju, L.; Zhou, J.; Zhang, Y.F. Conservation laws analysis of nonlinear partial differential equations and their linear soliton solutions and Hamiltonian structures. *Commun. Anal. Mech.* **2023**, *15*, 24–49. [CrossRef]
3. Şenol, M. Abundant solitary wave solutions to the new extended $(3+1)$–dimensional nonlinear evolution equation arising in fluid dynamics. *Mod. Phys. Lett. B* **2025**, *39*, 2450475. [CrossRef]
4. Mahmood, S.S.; Murad, M.A.; Emadifar, H.; Ahmed, K.K. Analysis of optical solitons, bifurcation, and chaos for the $(3+1)$–dimensional nonlinear evolution model. *Results Eng.* **2026**, *32*, 111962. [CrossRef]
5. Jia, Y.-H.; Si, Z.-Z.; Ju, Z.-T.; Feng, H.-Y.; Zhang, J.-H.; Yan, X.; Dai, C.-Q. Convolutional-recurrent neural network for the prediction of formation and switching dynamics for multicolor solitons. *Sci. China Phys. Mech. Astron.* **2025**, *68*, 284211. [CrossRef]
6. Hirota, R. *The Direct Method in Soliton Theory*; Cambridge University Press: Cambridge, UK, 2004.
7. Wang, M.; Wang, Y. A new Bäcklund transformation and multi-soliton solutions to the KdV equation with general variable coefficients. *Phys. Lett. A* **2001**, *287*, 211–216. [CrossRef]
8. Rani, A.; Ashraf, M.; Ahmad, J.; Ul-Hassan, Q.M. Soliton solutions of the Caudrey–Dodd–Gibbon equation using three expansion methods and applications. *Opt. Quant. Electron.* **2022**, *54*, 158. [CrossRef]
9. Ghanbari, B.; Inc, M. A new generalized exponential rational function method to find exact special solutions for the resonance nonlinear Schrödinger equation. *Eur. Phys. J. Plus* **2018**, *133*, 142. [CrossRef]
10. Gui, L.; Zhang, Y. Inverse scattering transform for the $(3+1)$–dimensional Zakharov–Kuznetsov equation. *Math. Methods Appl. Sci.* **2025**, *48*, 13622–13631. [CrossRef]
11. Baloch, S.A.; Raza, A.; Moyo, S. Lie symmetry analysis, rogue waves, periodic waves and various analytical solutions of non-linear diffusion equation with applications. *Nonlinear Dyn.* **2025**, *113*, 32649–32667. [CrossRef]
12. Özis, T.; Aslan, I. Application of the G'/G–expansion method to Kawahara type equations using symbolic computation. *Appl. Math. Comput.* **2010**, *216*, 2360–2365. [CrossRef]
13. Shang, Y. Abundant explicit non-traveling wave solutions for the $(2+1)$–dimensional breaking soliton equation. *Appl. Math. Lett.* **2022**, *131*, 108029. [CrossRef]
14. Vakhnenko, V.A. Solitons in a nonlinear model medium. *J. Phys. A Math. Gen.* **1992**, *25*, 4181–4187. [CrossRef]
15. Vakhnenko, V.O.; Parkes, E.J. Approach in theory of nonlinear evolution equations: The Vakhnenko–Parkes equation. *Adv. Math. Phys.* **2016**, *2016*, 6314058. [CrossRef]
16. Victor, K.K.; Thomas, B.B. On high frequency soliton solutions to a $(2+1)$–dimensional nonlinear partial differential evolution equation. *Chin. Phys. Lett.* **2008**, *25*, 425–428. [CrossRef]
17. Wazwaz, A. Two wave mode higher-order modified KdV equations. *Int. J. Numer. Methods Heat Fluid Flow* **2017**, *27*, 2223–2230. [CrossRef]
18. Wazwaz, A. Higher dimensional integrable Vakhnenko–Parkes equation: Multiple soliton solutions. *Int. J. Numer. Methods Heat Fluid Flow* **2021**, *31*, 2064–2071. [CrossRef]
19. Özkan, Y.S.; Seadawy, A.R.; Yaşar, E. Multi-wave, breather and interaction solutions to $(3+1)$–dimensional Vakhnenko–Parkes equation arising at propagation of high-frequency waves in a relaxing medium. *J. Taibah Univ. Sci.* **2021**, *15*, 666–678. [CrossRef]
20. Arshed, S.; Akram, G.; Sadaf, M.; Hussain, E.; Abbas, M.; Alzaidi, A.S.; Riaz, M.B. Investigation of the dynamical structures for nonlinear Vakhnenko–Parkes equation using two integration schemes. *Opt. Quantum Electron.* **2024**, *56*, 1072. [CrossRef]
21. Mehann, M.S.; Alazman, I.; Seadawy, A.R. Comprehensive study of a $(3+1)$–dimensional nonlinear Vakhnenko–Parkes dynamical equation with applications in nonlinear wave propagation in relaxing media. *AIMS Math.* **2025**, *10*, 25206–25226. [CrossRef]
22. Aslan, E.C.; Deniz, D.; Inc, M. Novel soliton solutions via the Nucci reduction and the extended direct algebraic methods: Chaotic dynamics and bifurcation analysis. *J. King Saud Univ. Sci.* **2026**, *38*, 19952025. [CrossRef]
23. Özkan, Y.S.; Yaşar, E.; Osman, M.S. Novel multiple soliton and front wave solutions for the 3D-Vakhnenko–Parkes equation. *Mod. Phys. Lett. B* **2022**, *36*, 2250003. [CrossRef]
24. Yin, Y.H.; Lü, X.; Ma, W.X. Bäcklund transformation, exact solutions and diverse interaction phenomena to a $(3+1)$–dimensional nonlinear evolution equation. *Nonlinear Dyn.* **2022**, *108*, 4181–4194. [CrossRef]
25. Alkinidri, M.; Alsallami, S.A. Abundant non-traveling fractal solutions of dromion type for the extended Hirota–Satsuma–Ito equation. *Fractal Fract.* **2026**, *10*, 356. [CrossRef]
26. Alsallami, S.A. On Exact Non-Traveling Wave Solutions to the Generalized Nonlinear Kadomtsev–Petviashvili Equation in Plasma Physics and Fluid Mechanics. *Mathematics* **2025**, *13*, 1914. [CrossRef]

Disclaimer/Publisher's Note: The statements, opinions and data contained in all publications are solely those of the individual author(s) and contributor(s) and not of MDPI and/or the editor(s). MDPI and/or the editor(s) disclaim responsibility for any injury to people or property resulting from any ideas, methods, instructions or products referred to in the content.